ISSN 1070-4272, Russian Journal of Applied Chemistry, 2016, Vol. 89, No. 3, pp. 421−431. © Pleiades Publishing, Ltd., 2016.
Original Russian Text © M.S. Voronov, V.N. Sapunov, A.A. Makarov, A.D. Kulazhskaya, E.S. Kaleeva, 2016, published in Zhurnal Prikladnoi Khimii, 2016, Vol. 89, No. 3, pp. 370−380.

PROCESSES USING VARIOUS CATALYST SYSTEMS

Improvement of a Process for Preparing Peracetic Acid by the Reaction of Acetic Acid with Hydrogen Peroxide in Aqueous Solutions, Catalyzed by Ion-Exchange Resins

M. S. Voronov, V. N. Sapunov*, A. A. Makarov, A. D. Kulazhskaya, and E. S. Kaleeva

Mendeleev Russian University of Chemical Technology, Miusskaya pl. 9, Moscow, 125047 Russia
**e-mail: sapunovvals@gmail.com*

Received March 1, 2016

Abstract—The effect of Amberlyst 15Dry™ cation-exchange resin on the reaction of peracetic acid formation from acetic acid and hydrogen peroxide in aqueous solution was studied. The pathways of available oxygen consumption were determined. The noncatalytic synthesis is accompanied by spontaneous decomposition of the peracid formed, which sharply decelerates on introducing Amberlyst 15Dry catalyst into the reaction mixture. Comparison of the kinetic relationships of the processes occurring in batch and flow-through reactors shows that in the latter case the process is characterized by diffusion hindrance. A kinetic model of the process with the parameters ensuring adequate mathematical description of the data obtained was suggested.

DOI: 10.1134/S1070427216030125

Peracetic acid (AcOOH) as the most accessible peracid has found wide use as versatile disinfectant [1, 2], bleaching agent [3], reagent for preparing various epoxy compounds [4], etc. Peracids are prepared in batch or continuous reactors in the presence of homogeneous (sulfuric acid) or heterogeneous (as a rule, various ion-exchange resins) acid catalysts [5]. The use of microreactors attracts attention, allowing implementation of the reaction unit to be simplified [6–9].

However, the use of inorganic acids as catalysts requires the use of corrosion-resistant materials. It seems more promising to use a reaction unit with a fixed bed of a heterogeneous catalyst, a cation-exchange resin. In flow-through reactors, the mechanical wear of the catalyst decreases and its operation life increases. The catalytic activity of ion-exchange resins decreases in the order Dowex 50W×2 > Smopex-101 > Dowex 50W×8 ≈ Amberlite IR-120 > Amberlyst 15Dry, which is associated with an increase in the degree of matrix cross-linking and a decrease in the accessibility of the ion-exchange sites [10]. In contrast to homogeneous catalysis, catalysis with ion-exchange resins is complicated by the effect of diffusion processes, which depend on the hydrodynamic conditions at the surface and in pores of the catalyst [5]. In stirred reactors, external diffusion hindrance is lifted at high rotation rates, ensuring high turbulence of the reaction mixture flow at the catalyst surface. The internal diffusion hindrance is manifested at the degree of support cross-linking of 8% and higher and/or at catalyst particle size larger than 0.3 mm [5, 10, 11]. Both types of diffusion hindrance considerably decrease when the reaction medium is subjected to ultrasonic treatment [9]. The influence of ultrasound is probably associated with intensification of the mass exchange at the surface and in pores of the catalyst.

By now, ample data have been accumulated in the literature on the mechanism of peracid formation. The reaction is considered as acid-catalyzed equilibrium reaction of an organic acid with hydrogen peroxide. The DFT calculations have shown that the step determining the reaction rate is the formation of a neutral tetrahedral intermediate [12].

A study of the kinetics and mechanism of peracetic acid formation from solutions of acetic acid (AcOH)

and hydrogen peroxide (H_2O_2) in the presence of orthophosphoric acid as stabilizer showed that the equilibrium constant depended neither on the reactant ratio nor on the catalyst (sulfuric acid) concentration varied within 0–9.0 wt % [13]. The rate constants of the forward and reverse reactions proportionally increase in the catalyst concentration interval 0–5 wt % and do not change further at the catalyst concentration increased to 9 wt %. Similar results were obtained in other studies for different types of reactors [6, 14] and with different amounts of a heterogeneous catalyst [5].

Unexpected results were obtained when analyzing data for the reaction of perpropionic acid formation, catalyzed by sulfuric acid. Namely, the equilibrium constant linearly increased with increasing catalyst concentration. This fact was attributed to the nonideality of the reaction system in the presence of a high concentration of a strong electrolyte (the molar concentration of sulfuric acid reached 1.41 M) [10]. Apparently, in this case the procedure for calculating the concentration of water as nonassociated medium cannot be used. Experimental studies (IR spectroscopy [15]) and calculations (DFT [16]) proved the presence of diverse hydrates or solvates, up to $H_2SO_4 \cdot 6H_2O$, in aqueous solutions of sulfuric acid. These species transform into each other after overcoming a definite energy barrier [17]. This means that the concentration of "free" water molecules participating in the equilibrium formation of peracids is considerably underestimated, which leads to overestimated values of the equilibrium constant and equilibrium concentration of the peracid.

Attainment of the equilibrium of peracetic acid formation is accompanied by a series of concurrent reactions with the release of oxygen or CO_2. Published data on transformations of available oxygen in the course of peracid synthesis give no clear views on the decomposition pathways of peroxy compounds [18, 19]. One of the first studies on the process kinetics showed that the peracid decomposition occurred as a second-order reaction. The isotope analysis allowed a conclusion that the released molecular oxygen is formed to 83% from the peroxy ($H^{18}O^{18}O$–) fragment of the peracid. The maximal decomposition rate is reached when the solution acidity corresponds to pK_a of peracetic acid. The results of that kinetic study were later confirmed in [18]. Initially the maximum in the dependence of the decomposition rate constant on the solution acidity was interpreted as corresponding to the reaction of the undissociated peracid species with its anion. However, Xuebing Zhao et al. [20], though confirming the revealed complex dependence of the peracetic acid decomposition rate on the solution acidity, believe that the rate-determining step is the reaction of the peracid molecule with its protonated form. The suggested decomposition mechanisms probably do not reflect the actual process adequately, because addition of complexones (phosphates, phosphoric acid) to the reaction mixture suppresses the decomposition [13]. It should be noted that, when obtaining a kinetic model of peracid formation, Leveneur et al. [5, 10] have not revealed the fact of peracid decomposition at all, although they used standard chemicals (Acros, Merck, Baker).

Detailed consideration of studies on the kinetics and mechanism of peracetic acid formation does not allow comparative analysis of data for the homogeneous and heterogeneous catalytic processes, because it is difficult to find fully comparable process conditions.

This study was aimed at comparative analysis of the kinetics of peracetic acid formation in batch and continuous reactors using a fixed bed of the catalyst (cation-exchange resins) and at elucidation of the pathways of available oxygen consumption.

EXPERIMENTAL

Acetic acid [glacial, GOST (State Standard) 61–65] and hydrogen peroxide (37 wt %, medical grade, GOST 177–88) were purchased from Khimmed. Amberlyst 15Dry™ ion-exchange resin (Rohm & Haas, France) was used as catalyst. It consisted of spherical particles 0.425 mm in diameter and had the following characteristics: concentration of acid sites (dry catalyst) 4.7 equiv kg^{-1}, bulk density 610 g L^{-1}, swellability 38%, pore diameter 30 nm (data obtained in accordance with ISO 9001).

For iodometric titration, we used a 0.1 N aqueous solution of sodium thiosulfate (Fixanal), potassium iodide (chemically pure grade, GOST 4232–77), and acetic acid, purchased from Khimmed. Potentiometric analysis was performed by titration with an aqueous potassium hydroxide solution (0.18 N) using an ATP-2 automatic potentiometric titrator (Akvilon, Russia). Potassium hydroxide (analytically pure grade, GOST 24363–80) was purchased from Khimmed.

The kinetic features of peracetic acid formation were studied under the conditions of batch and equilibrium

processes. We analyzed the results of experimental series performed with different molar ratio of the reactants ([AcOH] : [H_2O_2] from 1 : 6 to 5 : 1) at a constant sum of their volumes (45 mL for the batch process and 72 mL for the continuous process) and with different amounts of the catalyst in the temperature interval 25–80°C. The reaction progress was monitored by determining the content of hydrogen peroxide, acetic acid, and peracetic acid. Peracetic acid was analyzed simultaneously by methods of potentiometric acid–base titration and iodometric titration.

Batch process. The reaction kinetics under conditions of a batch process was studied in a 150-mL cylindrical glass reactor equipped with a power-driven stirrer, a temperature-control jacket, a reflux condenser, and a thermometer. Reflectors in the form of glass plates were mounted in the reactor to enhance the stirring intensity. The reactor was charged with the catalyst (when studying the catalytic process) and acetic acid, the mixture was heated to the required temperature, and a definite amount of hydrogen peroxide heated to the same temperature was added. The total volume of the liquid phase was 45 mL. The stirring rate was about 600 rpm. Samples for analysis of reaction products were taken at definite time intervals.

Continuous process. Experiments under the conditions of a continuous process were performed using a flow-through reactor in the form of a glass tube 16 mm in diameter and 200 mm long. The tube was equipped with a temperature-control jacket. The catalyst bed was arranged in the tube between glass wool layers placed in the lower and upper parts of the tube. The thickness of the glass wool layer in the upper part of the tube was 25–30 mm, which was sufficient for the starting mixture to be heated to the required temperature. The catalyst amount was 3–10 g. Prior to starting the reaction, 50 mL of distilled water was passed through the catalyst bed at a temperature of the subsequent experiment. After that, the calculated amounts of acetic acid and hydrogen peroxide solutions were mixed and fed to the reactor at a preset rate. To study the variation of the concentration with time, the mixture was repeatedly passed through the fixed bed of the catalyst. The products were analyzed by the same methods as for the batch process.

The process hydrodynamics (Reynolds number) for the liquid passing through a bed of spherical catalyst granules was calculated by the known formula

$$\mathrm{Re} = \frac{R_p G}{\mu}, \quad (1)$$

where R_p is the catalyst grain radius; G, gravimetric flow rate of the reaction mixture per unit area of the reactor cross section (kg s^{-1} m^{-2}); and μ, dynamic viscosity of the medium (Pa s).

Samples of the reaction mixture were taken directly from the reactor and analyzed. The acetic and peracetic acid concentrations were determined by potentiometric acid–base titration. For these acids, the potential jumps were in the intervals from 0 to 30 and from –130 to –100 mV, respectively. In addition, the content of peracid and hydrogen peroxide was determined by iodometric titration as described in [21]. The results of measuring the peracid concentrations by the two procedures were similar with the maximal deviation of 3.0–4.0 rel %.

RESULTS AND DISCUSSION

In the first step, we analyzed the ratios of the formed products and converted reactants excluding the reaction time (or contact time) as a process parameter. The result of this analysis is the scheme and sequence of product formation in the noncatalytic and catalytic reactions. Apparently, the noncatalytic reaction is actually the reaction catalyzed by acetic acid proton. In the next step, we determined the parameters of the rate equations corresponding to the suggested scheme. The equation parameters were found by the traditional method from the dependences of the concentrations of the reactants and reaction products on the reaction time (or contact time).

Noncatalytic Reaction

The series of experiments on noncatalytic synthesis of peracetic acid were performed in the temperature interval 50–80°C at the initial reactant concentrations, $[H_2O_2]_0$ and $[AcOH]_0$, of 4.22 and 12 M, respectively. Analysis of the reaction mixture in the course of the reaction showed that the sum of the running concentrations of acetic and peracetic acids, $\{[AcOH]_i + [AcOOH]_i\}$, remained constant. However, the sum of the running concentrations of hydrogen peroxide and peracetic acid, $\{[H_2O_2]_i + [AcOOH]_i\}$ (i.e., the concentration of available oxygen, $[O]_i$), decreased in the course of the reaction. Figure 1 illustrates the revealed relationships. For these correlations, instead of the reaction time we

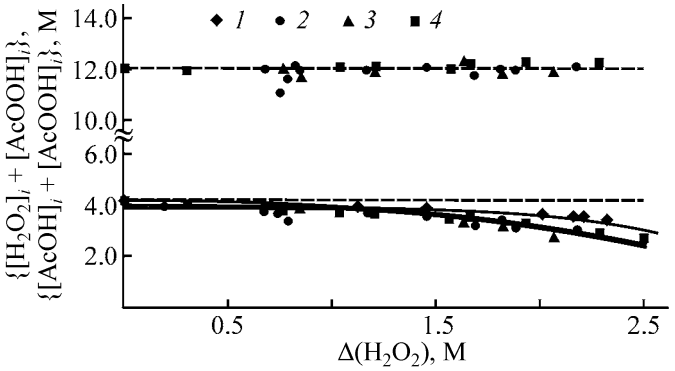

Fig. 1. Correlation of the sum of the running concentrations $\{[AcOH]_i + [AcOOH]_i\}$ (upper points) and $\{[H_2O_2]_i + [AcOOH]_i\}$ (lower points) with the change in the hydrogen peroxide concentration, $\Delta(H_2O_2) = \{[H_2O_2]_0 - [H_2O_2]_i\}$, for the reactions performed in the temperature interval 50–80°C. The lines are the results of calculations using the mathematical model of the process [Eqs. (3)–(7)]; the same for Fig. 2. *T*, °C: (*1*) 50, (*2*) 60, (*3*) 70, and (*4*) 80; the same for Fig. 2.

chose the change in the hydrogen peroxide concentration ($\Delta[H_2O_2]$, M) by the given time moment.

Because the sum of the acids, $\{[AcOH]_i + [AcOOH]_i\}$, does not noticeably change in the course of the reaction, we can conclude that reaction in our experiments does not involve "skeletal" decomposition of the peracid to CO_2, as found previously for performic acid [22]. On the other hand, the available oxygen concentration decreases as hydrogen peroxide is consumed. This fact suggests the decomposition of peroxy compounds, increasing with temperature. The uncertainty in determination of the initial slope in this correlation does not allow unambiguous conclusions on the possible decomposition of H_2O_2, because

$$\left(\frac{d[O]_i}{d[H_2O_2]}\right)_{t\to 0} \approx 0. \qquad (2)$$

The nonproportional increase in the loss of available oxygen in the reaction mixture with the progress of the reaction suggests the occurrence of the peracid decomposition:

$$2AcOOH \rightarrow 2AcOH + O_2.$$

This trend is illustrated by Fig. 2, which shows how the selectivity of peracetic acid formation with respect to hydrogen peroxide changes in the course of the reaction. The initial portions of the approximating curves virtually coincide with the line corresponding to 100% selectivity. The selectivity decreases with the consumption of hydrogen peroxide, and as the reaction temperature is increased to 80°C, the selectivity decreases to approximately 50%. These facts suggest that the peracid decomposition makes the major contribution to the loss of available oxygen.

Thus, the correlations obtained do not give unambiguous information on the decomposition pathways of the peroxy compounds. Their elucidation requires more detailed mathematical analysis of the results obtained.

The correlations considered are consistent with the generalized scheme of the noncatalytic reaction of peracetic acid formation:

$$\begin{array}{ccc} AcOH + H_2O_2 & \underset{k_2}{\overset{k_1}{\rightleftharpoons}} & AcOOH + H_2O_2 \\ \downarrow k_{30} & & \downarrow k_{31} \\ H_2O + 1/2O_2 & & AcOH + 1/2O_2 \end{array}$$

The following system of differential equations corresponds to this scheme:

$$-\frac{d[H_2O_2]}{dt} = k_1[AcOH][H_2O_2] - k_2[AcOOH][H_2O] - k_{30}[H_2O_2], \qquad (3)$$

$$-\frac{d[AcOH]}{dt} = k_1[AcOH][H_2O_2] - k_2[AcOOH][H_2O] - k_{31}[AcOOH]^n, \qquad (4)$$

$$-\frac{d[AcOH]}{dt} = k_1[AcOH][H_2O_2] - k_2[AcOOH][H_2O] - k_{31}[AcOOH]^n, \qquad (5)$$

$$-\frac{d[H_2O]}{dt} = k_1[AcOH][H_2O_2] - k_2[AcOOH][H_2O], \qquad (6)$$

$$-\frac{d[O_2]}{dt} = 1/2k_{31}[AcOOH]^n, \qquad (7)$$

Table 1. Results of mathematical modeling of noncatalytic synthesis of peracetic acid at $[AcOH]_0 = 12$, $[H_2O_2]_0 = 4$ M in the temperature interval 50–80°C

T, °C	$k_1 \times 10^4$	$k_2 \times 10^4$	$k_{31} \times 10^3$	K_{eq}
	L min^{-1} mol^{-1}			
50	1.02	0.35	0.25	2.9
60	1.22	0.45	1.8	2.7
70	2.81	1.1	5.5	2.55
80	5.39	2.2	11	2.45
50–80	$7.05 \times 10^4 \exp(-6635.1/T)$	$1.8 \times 10^5 \exp(-7279.4/T)$	$5.72 \times 10^{15} \exp(-14310/T)$	$0.393 \exp(644.3/T)$
R^2	0.94	0.95	0.96	0.99

where k_1 and k_2 are the rate constants of the forward and reverse reactions of peracid formation, k_{30} and k_{31} are the rate constants of the decomposition of hydrogen peroxide and peracid, and n is the order of the peracid decomposition reaction.

The scheme was refined and the numerical values of the parameters of the differential equations were obtained by the least-squares method with respect to the concentrations of hydrogen peroxide, acetic acid, and peracetic acid. The water concentration was calculated from the sum of the amounts of water introduced with the solution ($[H_2O_2]_0$) and formed by perhydrolysis [Eq. (6)].

Modeling of the reaction system by Eqs. (3)–(7) has shown that constant k_{30} is statistically insignificant. The best fit of the experimental reactant concentrations is reached at $k_{30} = 0$, $n = 2$. In this case, the approximation reliability (R^2) for the linear regression of all the experimental and calculated values of $[AcOH]_i$, $[H_2O_2]_i$, and $[AcOOH]_i$ in one experiment was $R^2 = 0.98$. The results obtained, including the calculated equilibrium constant K_{eq}, are given in Table 1.

All the parameters of the mathematical model, including the second order of the peracid decomposition reaction ($n = 2$), reasonably agree with the corresponding values from the literature [13]. Slight deviations observed when comparing the numerical values can be attributed to differences in the experimental conditions. For example, the presence of phosphoric acid in the reaction mixture as stabilizer [13] or different initial concentrations of acetic acid in the process affect the proton concentration, and the functional dependence on this quantity is included in constants k_1 and k_2 [14, 20]. The presence of stable acetic acid hydrates in the reaction mixture, affecting the concentration of "free" water, should also be taken into account [23]. Formally this leads to an increase in the calculated value of the equilibrium constant, determined as the ratio $K_{eq} = k_1/k_2$. Neglect of the change in the water concentration due to its incorporation in various solvates leads to incorrect interpretation of the temperature dependence of the equilibrium constant. Some authors report its increase with temperature [24], whereas other authors report its decrease [13]. According to our data, the equilibrium constant of the noncatalytic reaction decreases with increasing temperature (Table 1). The mathematical description of the noncatalytic synthesis of peracetic acid

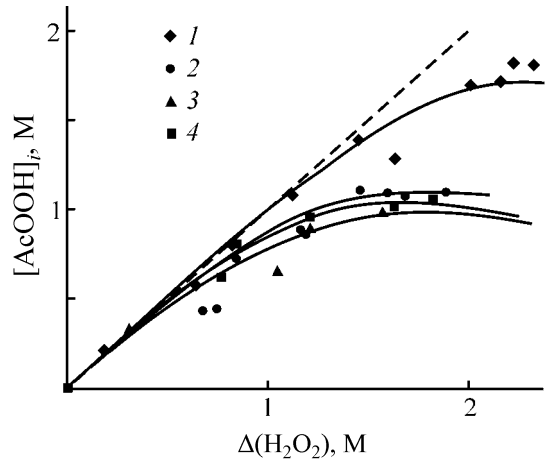

Fig. 2. Correlation of the running concentration of peracetic acid $[AcOOH]_i$ with the change in the hydrogen peroxide concentration, $\Delta(H_2O_2) = \{[H_2O_2]_0 - [H_2O_2]_i)\}$ for the reactions performed in the temperature interval 50–80°C.

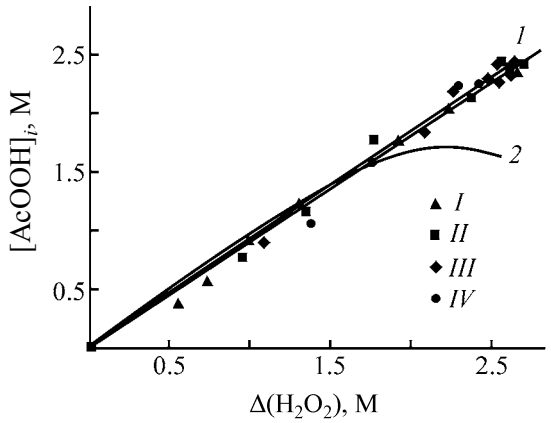

Fig. 3. Correlation of the concentrations of the peracid formed and hydrogen peroxide consumed at different amounts of the catalyst in the reaction mixture. (*1*) Catalytic reaction, catalyst amount, wt %: (*I*) 2, (*II*) 4, (*III*) 7, and (*IV*) 10; (*2*) noncatalytic reaction.

was subsequently used as a comparative model for the catalytic process.

Catalytic Reaction

To determine the relationships of the catalytic synthesis of peracetic acid in the presence of a catalyst ([cat], Amberlyst 15Dry), we performed experiments in batch and continuous reactors.

Batch process. To analyze the batch process, we performed three series of experiments in which we varied the catalyst amount (T = 50°C; $[H_2O_2]_0$ = 4.0, $[AcOH]_0$ = 12.0 M), reactant ratio (T = 50°C, [cat] = 7 wt %), and reaction temperature ([cat]= 7 wt %; $[H_2O_2]_0$ = 4.0, $[AcOH]_0$ = 12.0 M).

The stirrer rotation rate required to eliminate the effect of external diffusion factors was determined in preliminary experiments. To this end, we performed a series of experiments with the stirrer rotation rate varied in the range 100–600 rpm. As we found, in the presence of the maximal amount of the catalyst (10 wt %) at stirrer rotation rates higher than 350 rpm, the kinetic curves of the H_2O_2 consumption and peracid formation fully coincided with each other, proving the absence of external diffusion hindrance. For further experiments performed with different amounts of the catalyst, we chose the stirrer rotation rate of 500 rpm.

Analysis of the reaction mixture from the first two series of experiments showed that the sum of the running acid concentrations, $\{[AcOH]_i + [AcOOH]_i\}$, remained constant in the course of the reaction, as in the previous noncatalytic experiments. However, in contrast to the noncatalytic process, the available oxygen concentration $[O]_i$ decreased in the course of the reaction only slightly. The results of processing the data from several experiments with different amounts of the catalyst are shown in Fig. 3. This correlation demonstrates the selectivity of the catalytic reaction of the AcOOH formation, which is independent of the catalyst amount (within random uncertainty).

Statistical treatment of the correlation between the concentrations of the peracid formed and hydrogen acid consumed, performed for the same series of experiments, revealed linear correlation between these quantities:

$$[AcOOOH]_i = (0.91 \pm 0.01)([H_2O_2]_0 - [H_2O_2]_i). \quad (8)$$

The linear regression obtained is characterized by R^2 values as high as 0.99 for all the experiments. Apparently, the catalyst does not significantly influence the peracid decomposition against the background of considerable acceleration of the target reaction. This hypothesis is confirmed by the conclusions made in some papers that no decomposition of hydrogen peroxide and peracetic acid was observed at temperatures lower than 55–60°C [5, 20].

Similar analysis of the selectivity, based on data of a series experiments at different reaction temperatures (25–80°C), did not reveal any trends. Statistical processing of the data revealed only the linear correlation similar to Eq. (8), but with somewhat lower approximation quality: R^2 = 0.98.

For further elucidation of the kinetic relationships of the catalytic reaction, we performed more detailed mathematical analysis of the results obtained. We chose for the modeling the above-given reaction scheme and the corresponding system of Eqs. (3)–(7). Refinement of the scheme and determination of the numerical values of the differential equation parameters were performed, as in the previous case, by the least-squares method. The best fit of the experimental reactant concentrations in all the experimental series was obtained at k_{30} = 0 and n = 2. In this case, the linear regression of the experimental and calculated values of $[AcOH]_i$, $[H_2O_2]_i$, and $[AcOOH]_i$ was characterized by R^2 = 0.99. The results are given in Table 2.

As expected, the rate constants of the forward and reverse reactions are linear functions of the catalyst amount in the reaction mixture ([cat]):

$$k_1 = (1.0 + 1.6[\text{cat}]) \times 10^{-4}\ \text{L mol}^{-1}\ \text{min}^{-1}, \quad (9)$$

$$k_2 = (0.35 + 0.5[\text{cat}]) \times 10^{-4}\ \text{L mol}^{-1}\ \text{min}^{-1}, \quad (10)$$

where [cat] is the catalyst amount in the reaction solution (%).

The absolute term in Eqs. (9) and (10) corresponds to the rate constant of the noncatalytic reaction. Taking into account high approximation reliability ($R^2 \approx 0.99$) for the linear regressions obtained for constants k_1 and k_2, slight fluctuations in the calculated values of the equilibrium constant should be considered as an artifact. A different pattern, however, is observed in the influence of temperature on K_{eq} in the noncatalytic and catalytic processes. In the first case, the equilibrium tends to be shifted to the left (Table 1), whereas in the presence of the catalyst the equilibrium constant does not change noticeably (Table 2). This phenomenon may be due to a decrease in the water concentration at the reaction site as a result of its sorption by the relatively large amount (up to 10 wt %) of the catalyst.

Comparison of the kinetic constants given in Tables 1 and 2 shows that the presence of the catalyst alters the relationships of the peracetic acid decomposition. Whereas at 50°C the values of k_{31} coincide in both processes, with increasing temperature they become different. In the catalytic process, the constant k_{31} increases with temperature considerably more slowly. In addition, the peracid decomposition constant sharply decreases with increasing catalyst amount in the reaction mixture. This phenomenon is consistent with conclusions of some authors that the peracid does not decompose under the conditions of acid catalysis (including catalysis with ion-exchange resins) [5, 10].

The decrease in the rate of spontaneous decomposition of peracetic acid with increasing catalyst concentration allowed speaking of the acid stabilization of the peracid solution. The rate constant of the peracid decomposition is a fractional-linear function of the proton concentrationa [20]. Indeed, variation of the rate constant k_{31} with increasing catalyst amount (Table 2) is described by a similar equation with very high approximation reliability ($R^2 = 0.989$):

$$k_{31} = \frac{3.5 \times 10^{-4}(\alpha + [\text{cat}])}{0.3 + (\alpha + [\text{cat}])^2},\ \text{L mol}^{-1}\ \text{min}^{-1}, \quad (11)$$

where [cat] is the catalyst amount in the reaction mixture (%); α, empirical equivalent of the solution acidity

Table 2. Parameters of the kinetic model of peracetic acid synthesis catalyzed by Amberlyst 15Dry [system of Eqs. (3)–(7)] in the batch mode

T, °C	[cat], wt %	$k_1 \times 10^4$	$k_2 \times 10^4$	$k_{31} \times 10^3$	K_{eq}
		L min^{-1} mol^{-1}			
50	0	1.02	0.35	2.4	2.9
50	2[a]	4.7	1.5	1.2	3.1
50	4	7.5	2.4	0.7	3.1
50	7	12	3.9	0.42	3.1
50	10	17	5.3	0.25	3.2
25	7	4.8	1.5	0.1	3.2
50	7	12	3.9	0.35	3.1
65	7	28	9.2	0.9	3.0
80	7	46	15.5	1.2	3.0
25–80	7	1182.4exp(–4406.8/T)	589.1exp(–4545.8/T)	173.3exp(–4963.2/T)	
R^2		0.99	0.99	0.98	

[a] The constants given for this experiment described all the kinetic curves at the reactant ratio $[AcOH]_0 : [H_2O_2]_0$ varied in the interval from 5 : 1 to 1 : 1.

without catalyst, equal to 0.1 in our case; and (α + [cat]), empirical equivalent of the proton concentration {Eq. (29) in [20]}.

Thus, the mathematical model of the process in the form of the system of differential equations (3)–(7) with the corresponding parameters fully describes the peracetic acid formation both in the presence of the catalyst and without it.

Continuous process. To compare the results of modeling of the heterogeneous-catalytic reaction under conditions of the batch and continuous processes, it was necessary to choose common time units. Related processes are often described using such quantity as the residence time, defined as quotient from division of the void volume of the reactor by the volumetric rate of feeding the reaction mixture [8, 9]. However, the time calculated by this procedure cannot be directly used in our case. To describe the heterogeneous-catalytic process under consideration, we can use such a commonly accepted term as "conventional contact time" τ of the reaction mixture with the catalyst:

$$\tau = \frac{[\text{cat}]}{Q}, \text{ min } g_{\text{catalyst}}\, mL^{-1}_{\text{reaction mixture}}, \qquad (12)$$

where [cat] is the catalyst weight in the reactor (g), and Q is the amount of the starting mixture fed in unit time (mL min^{-1}).

The conventional contact time τ can be formally interpreted as the contact time of the unit volume of the reaction mixture with the whole amount of the catalyst. In this case, we can easily compare the parameters of the continuous and batch processes, because for the latter process

$$\tau = \frac{[\text{cat}]}{V} t, \text{ min } g_{\text{catalyst}}\, mL^{-1}_{\text{reaction mixture}}, \qquad (13)$$

where [cat] is the catalyst weight in the reactor (g), V is the reaction mixture volume in the reactor (mL), and, t is the running reaction time (min).

In our case, the results of calculations using the conventional contact time τ can be appreciably distorted because of the noncatalytic reaction occurring simultaneously. It is more appropriate to use the quantity τ* proportional to the residence time of the reaction solution in the reactor and calculated as the reciprocal volumetric rate of feeding the reaction mixture, Q:

$$\tau^* = \frac{1}{Q}, \text{ min } mL^{-1}_{\text{reaction mixture}}. \qquad (14)$$

The quantity τ* can be interpreted as conventional contact time corresponding, e.g., to the time in which unit volume of the reaction mixture passes through the cross section of the flow-through reactor. Multiplication of this quantity by such constant parameters as the void volume or catalyst weight in the catalytic reactor leads to the above-described known terms.

Introduction of time τ* allows mathematical description of the kinetics of the simultaneously occurring catalytic and noncatalytic reactions. The determined rate constants will be functions of the catalyst weight [e.g., Eqs. (9) and (10)]. In this case, we can use for modeling the process in the continuous reactor the system of Eqs. (3)–(7) with the replacement of t by τ* and of the rate constants k_1 and k_2 by a $k_{1\Sigma}$ and $k_{2\Sigma}$, respectively.

To compare the numerical values of the rate constants of the batch and continuous processes, it is sufficient to divide the running reaction time t of the batch process by the reaction mixture volume; the result will correspond to the time τ*.

The continuous process was analyzed in four series of experiments in which we varied the catalyst amount (T = 50°C; $[H_2O_2]_0$ = 7.31, $[AcOH]_0$ = 7.31 M; feeding rate 1 mL min^{-1}), rate of feeding the reaction mixture into the reactor (T = 50°C; [cat] = 5 g; $[H_2O_2]_0$ = 7.31, $[AcOH]_0$ = 7.31 M), reactant ratio $[AcOH]_0$: $[H_2O_2]_0$ in the interval from 1 : 1 to 1 : 6 (T = 50°C, [cat] = 7 g, feeding rate 2.85 mL min^{-1}), and reaction temperature ([cat]= 5 g; $[H_2O_2]_0$ = 7.31, $[AcOH]_0$ = = 7.31 M; feeding rate 1 mL min^{-1}).

Analysis of the reaction mixture from the series of experiments showed that the sum of the running acid concentrations {$[AcOH]_i$ + $[AcOOH]_i$} remained constant in the course of the reaction. As in the case of the batch process, the best fit of the experimental reactant concentrations was obtained at k_{30} = 0 and n = 2. The factor R^2 for the linear regression of the experimental and calculated values of $[AcOH]_i$, $[H_2O_2]_i$, and $[AcOOH]_i$ was as high as 0.99. The results are given in Table 3.

The relationships obtained in modeling of the continuous process appeared to be similar to those found for the batch process. As expected, an increase in the catalyst weight in the reactor led to a proportional

Table 3. Parameters of the kinetic model of the peracetic acid synthesis catalyzed by Amberlyst 15Dry [system of Eqs. (3)–(7)] in a flow-through reactor

T, °C	[cat], g	Feeding rate, mL min^{-1}	$k_{1\Sigma}$	$k_{2\Sigma}$	k_{31}	K_{eq}
			L mol^{-1} τ*$^{-1}$			
50	0	–	0.0046	0.0015	–	3.1
50	3	1	0.016	0.007	0.001	2.3
50	5	1	0.026	0.012	0.003	2.2
50	7	1	0.038	0.018	0.003	2.1
50	10	1	0.047	0.023	0.003	2.0
50	5	1	0.026	0.012	0.003	2.2
50	5	1.65	0.029	0.013	0.003	2.2
50	5[a]	2.85	0.034	0.014	0.003	2.4
50	5	4	0.038	0.0155	0.003	2.5
40	5	1	0.02	0.01	0.002	2
50	5	1	0.026	0.012	0.003	2.2
60	5	1	0.032	0.014c	0.004	2.3
40–60	5	1	50.93exp(–2453.8/T)	2.73exp(–1756.1/T)	213.5exp(–3620.8/T)	18.63exp(–697.8/T)
R^2			0.988	0.999	0.994	0.99

[a] The constants given for this experiment described all the kinetic curves at the reactant ratio $[H_2O_2]_0$: $[AcOH]_0$ varied in the interval from 6 : 1 to 1 : 1.

increase in the rate constants of the forward and reverse reactions, k_1 and k_2:

$$k_{1\Sigma} = (0.0036 + 0.0045\ [cat])\ \text{L mol}^{-1}\ \tau^{*-1}, \quad (15)$$

$$k_{2\Sigma} = (0.0015 + 0.0023\ [cat])\ \text{L mol}^{-1}\ \tau^{*-1}, \quad (16)$$

where [cat] is the catalyst weight in the reactor (g).

However, the calculated rate constants appeared to be considerably lower than the corresponding quantities for the batch process, recalculated to time τ* in accordance with Eq. (14). For example, for the batch process in the presence of 10% catalyst (5 g, Table 2), the constants k_1 and k_2 are 0.075 and 0.024 L mol^{-1} τ*$^{-1}$, respectively. However, the rate constants of the continuous process under the same conditions and with the same amount of the catalyst, according to Eqs. (15) and (16), appeared to be considerably lower: 0.026 and 0.012 L mol^{-1} τ*$^{-1}$, respectively. With increasing volumetric rate of feeding the solution into the reactor, i.e., with increasing linear flow velocity, the rate constants increase also. Such variation of the constants is associated with manifestation of the diffusion processes whose significant contribution is confirmed by low activation energies of the forward and reverse reactions (Table 3).

The mathematical expression for the effect of diffusion on the process under consideration can be obtained assuming the additivity of the chemical and diffusion resistance. To this end, it is necessary to assume that the diffusion rate constant is directly proportional to the volumetric rate of feeding the reaction solution into the reactor:

$$k_{1\Sigma} = \frac{k_1(k_{1d}Q)}{[k_1 + k_{1d}Q)]}, \text{ L mol}^{-1}\ \tau^{*-1}, \quad (17)$$

$$k_{2\Sigma} = \frac{k_2(k_{2d}Q)}{[k_2 + k_{2d}Q)]}, \text{ L mol}^{-1}\ \tau^{*-1}, \quad (18)$$

where $k_{1\Sigma}$ is the overall rate constant of the forward reaction under kinetic control; $k_{2\Sigma}$, overall rate constant of the reverse reaction under kinetic control; k_{1d}, effective rate constant of diffusion of the reactants to the catalyst surface; k_{2d}, effective rate constant of the diffusion of the reaction products from the catalyst surface; and Q, volumetric rate of feeding the reaction mixture into the reactor (mL min^{-1}).

Indeed, at $k_{1d} = 0.02$ and $k_{2d} = 0.013$ [M τ^{*-1} (min mL^{-1})], we were able to reach high approximation reliability ($R^2 = 0.98$ and $R^2 = 0.95$) for the linear regression of all the experimental and calculated [Eqs. (17) and (18)] reaction rate constants. It should be noted that, at the volumetric rate of feeding the reaction mixture higher than 30 mL min^{-1}, the reaction should be kinetically controlled.

Indeed, calculation of the hydrodynamics in the bed of the spherical catalyst granules shows that, when the liquid passes through the bed of Amberlyst 15Dry catalyst at a low volumetric flow rate (1–4 mL min^{-1}, Table 3), the Reynolds number varies within 0.03–0.12, which corresponds to the laminar flow, whereas the maximal calculated rate would correspond to the turbulent flow with Re ≈ 100.

Experiments on continuous synthesis of peracetic acid revealed no relationships in the peracid decomposition. The rate constant k_{31} remained virtually constant in all the experiments.

CONCLUSIONS

The results of studying the main kinetic relationships of the formation of peracetic acid from standard solutions of acetic acid and aqueous hydrogen peroxide in the presence of Amberlyst 15Dry ion-exchange resin showed that two reactions (catalyzed by acetic acid and by the cation exchanger) occur simultaneously. The concurrent reaction is decomposition of the peracid via reaction of its protonated and nonprotonated species. The presence of the cation-exchange resin in the reaction system apparently increases the fraction of the protonated form, which leads to a decrease in the decomposition rate, i.e., the peracid is stabilized by the cation-exchange resin. The highest rate of the main reaction of the peracid formation was reached when performing the process in a batch reactor. In continuous synthesis of peracetic acid on a fixed catalyst bed, the process is hindered by slow diffusion of the reactants to the catalyst surface. The diffusion hindrance can be eliminated by increasing the flow rate to the level corresponding to turbulent hydrodynamics (Reynolds number Re > 100).

ACKNOWLEDGMENTS

The authors are grateful to the Russian Foundation for Basic Research and to the Ministry of Education and Science of the Russian Federation (task no. 4.2512.2014/K) for the financial support.

REFERENCES

1. Beber de Souza, J., Queiroz Valdez, F., Felipe Jeranoski, R., et al., *Int. J. Photoenergy*, 2015, vol. 2015, pp. 1–7.
2. Asensio, E., Sanagustín, F., Nerín, C., et al., *J. Chem*., 2015, vol. 2015, pp. 1–7.
3. Špička, N. and Tavčer, P.F., *Textile Res. J.,* 2015, vol. 85, no. 14, pp. 1497–1505.
4. Tan, S.G. and Chow, W.S., *Polym.–Plast. Technol. Eng*., 2010, vol. 49, pp. 1581–1590.
5. Leveneur, S., Warnå, J., Salmi, T., et al., *Chem. Eng. Sci.,* 2009, vol. 64, pp. 4101–4114.
6. Ebrahimi, F., Kolehmainen, E., Oinas, P., et al., *Chem. Eng. J*., 2011, vol. 167, pp. 713–717.
7. Kockmann, N., Gottsponer, M., and Roberge, D.M., *Chem. Eng. J*., 2011, vol. 167, no. 2, pp. 718–726.
8. Ebrahimi, F., Kolehmainen, E., and Turunen, I., *Chem. Eng. J*., 2012, vol. 179, pp. 312–317.
9. Jolhe, P.D., Bhanvase, B.A., Patil, V.S., and Sonawane, S.H., *Chem. Eng. J*., 2015, vol. 276, pp. 91–96.
10. Leveneur, S., Murzin, D.Y., Salmi, T., et al., *Chem. Eng. J*., 2009, vol. 147, no. 2, pp. 323–329.
11. Wärnå, J., Rönnholm, M.R., Salmi, T., and Keikko, K., *Chem. Eng. J*., 2002, vol. 90, no. 1, pp. 209–212.
12. Rubio, M., Ramırez-Galicia, G., and Jovany Lopez-Nava, L., *J. Mol. Struct.: Theochem*, 2005, vol 726, pp. 261–269.
13. Dul'neva, L.V. and Moskvin, A.V., *Russ. J. Gen. Chem*., 2005, vol. 75, no. 7, pp. 1125–1130.
14. Xuebing Zhao, Ting Zhang, Yujie Zhou, and Dehua Liu, *J. Mol. Catal. A: Chemical*, 2007, vol. 271, pp. 246–252.

15. Karen, L., Nash, K., Sully, J., and Horn, A.B., *Phys. Chem. Chem. Phys*., 2000, vol. 2, pp. 4933–4940.
16. Al Natsheh, A., Nadykto, A.B., Mikkelsen, K.V., et al., *J. Phys. Chem. A*, 2004, vol. 108, pp. 8914–8929.
17. Zeleznik, F.J., *J. Phys. Chem. Ref. Data*, 1991, vol. 20, no. 6, pp. 1157–1200.
18. Yuan, Z., Ni, Y., and van Heiningen, A.R.P., *Can. J. Chem. Eng*., 1997, vol. 75, pp. 37–41.
19. Yuan, Z., Ni, Y., and van Heiningen, A.R.P., *Can. J. Chem. Eng*., 1997, vol. 75, pp. 42–47.
20. Xuebing Zhao, Keke Cheng, Junbin Hao, and Dehua Liu, *J. Mol. Catal. A: Chemical*, 2008, vol. 284, pp. 58–68.
21. Dudley Sully, B. and Williams, P.L., *Analyst*, 1962, vol. 87, pp. 653–657.
22. Filippis, P. de, Scarsella, M., and Verdone, N., *Ind. Eng. Chem. Res*., 2009, vol. 48, pp. 1372–1375.
23. Liang Pu, Yueming Sun, and Zhibing Zhang, *J. Phys. Chem. A*, 2010, vol. 114, no. 40, pp. 10842–10849.
24. Musante, R.L., Grau, R.J., and Baltanas, M.A., *Appl. Catal. A: General*, 2000, vol. 197, pp. 165–173.